Article

Effects of Relative Density and Grading on the Particle Breakage and Fractal Dimension of Granular Materials

Gui Yang * , **Zhuanzhuan Chen, Yifei Sun and Yang Jiang**

Key Laboratory of Ministry of Education for Geomechanics and Embankment Engineering,
College of Civil and Transportation Engineering, Hohai University, Nanjing 210024, China;
czzjya@163.com (Z.C.); sunsunyifei@126.com (Y.S.); m18251975654@163.com (Y.J.)
* Correspondence: ygheitu@163.com

Abstract: Particle breakage was reported to have great influence on the mechanical property of granular materials. However, limited studies were conducted to quantify the detailed effects of relative density and initial grading on the particle breakage behaviour of granular materials under different confining pressures. In this study, a series of monotonic drained triaxial tests were performed on isotropically consolidated granular materials with four different initial gradings and relative densities. It is observed that particle breakage increases as the confining pressure or relative density increases, whereas it decreases with the increasing coefficient of uniformity. Due to particle breakage, the grading curves of granular materials after triaxial tests can be simulated by a power-law function with fractal dimension. As the confining pressure increases, the fractal dimension approaches the limit of granular materials, i.e., 2.6. A unique normalized relation between the particle breakage extent and confining pressure by considering relative density and grading index was found.

Keywords: granular materials; fractal dimension; particle breakage; relative density; grading curve

1. Introduction

Owing to the convenience of lower procurement cost, good compaction ability and high shear strength, granular materials have been widely used in hydraulic engineering, civil engineering and transport engineering, among others [1,2].

Due to the development of the rolling equipment technology, various types and grades of granular materials have been used for engineering construction, where the compactness of granular materials has been significantly improved, which effectively reduced the deformation of engineering facilities, e.g., a rockfill dam [3]. In a rockfill dam, granular materials often account for 60–90% of the total filling volume. Therefore, the strength and deformation of rockfill has an important impact on the stability and deformation analysis. However, upon external loading, significant particle breakage of granular materials can occur, which would have an important impact on the stability and deformation of the engineering facilities during both construction and operating periods. In particular, the grading curve changed evidently before and after loading [4]. Such degradation behaviour of granular materials was found to depend not only on stress history [5,6], but also on grain size distribution curve [7,8], parent rock type, particle size [9,10], particle shape [11,12] and relative density [13,14]. For example, particle shape has a significant influence on the particle breakage, which increases with the increasing in shape index sphericity, aspect ratio, convexity and overall regularity [12]. The critical state parameters (M, ϕ_{cs}, e_{Γ}, and λ_c) decrease with increasing aspect ratio, sphericity and convexity [8].

The relative density and grading curve are important control indicators at engineering site, e.g., the relative density of sand should be at least 0.70 [15]. It was also found to have a great influence on the shear strength and deformation of granular materials. The greater the relative density, the greater the initial elastic modulus and peak friction angle and

the smaller the volume strain [16,17]. However, previous studies mainly focused on the effect of strength and deformation of granular materials [18,19]. The fundamental physical properties that trigger particle breakage were not investigated in depth. For example, at large relative density, the stress–strain relationship usually exhibited strain softening. The stress–strain curve exhibited strain hardening with the decrease of relative density. The effect of initial void ratio on the stress–strain relationship decreases with increasing confining pressure [20,21]. With the increase in confining pressure, the difference of initial void decreases and reaches essentially the same value [20]. The residual strength of rockfill at different relative density was observed to be the same [22]. The critical state parameters (M and λ_c) are less affected by relative density and particle grading [7,13]. However, the critical state parameters (e_Γ) decrease with increasing relative density. The relative breakage index decreases with increasing relative density [14]. Extensive research has also been carried out on the impact of granular materials particle gradation [23–25]. For example, model parameters varied linearly with the coefficient of uniformity. The larger the coefficient of uniformity, the smaller the peak intensity and the larger volumetric strain.

In this study, a comprehensive study on the effect of relative density and initial grading on the particle breakage behavior of granular materials will be carried out, by using drained triaxial tests. An attempt is also made to propose a unique normalized relation between the particle breakage extent, applied pressure, relative density and grading index. The research results play an important role in understanding and mastering the gradation change law and strength characteristics of granular materials before and after loading, and provide an important reference for the stable design parameters of the structure.

2. Laboratory Tests

The granular materials, as shown in Figure 1, were collected from a quarry near Nanjing, China. Aggregates were derived from the parent of sandstone rock. The grain size distribution of the material and triaxial apparatus are shown in Figure 2. The dry density, coefficient of uniformity (C_u) and curvature coefficient (C_c) are listed in Table 1.

Figure 1. Test materials.
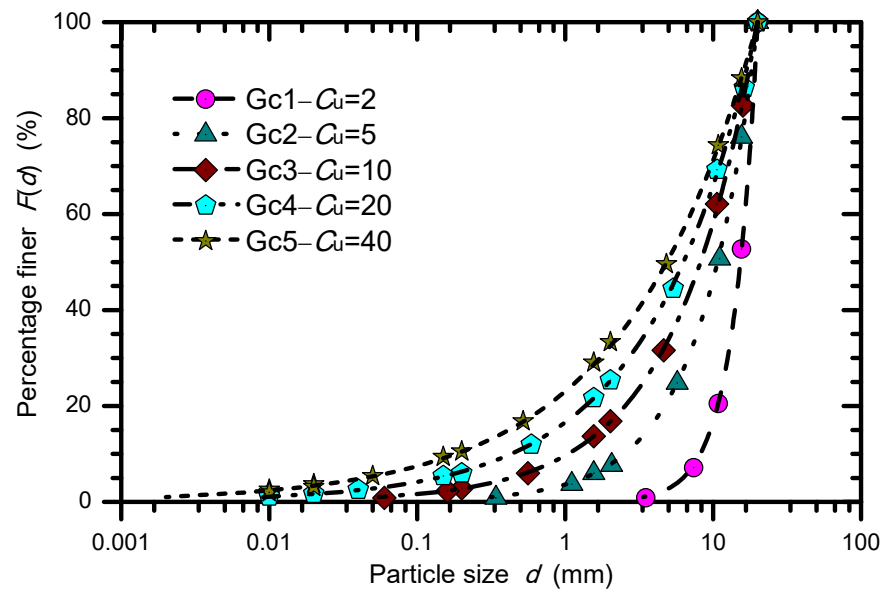
(**a**)
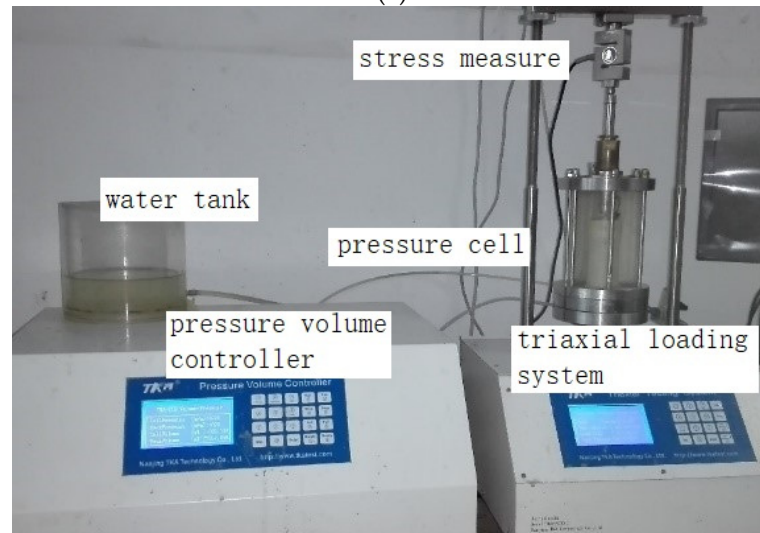
(**b**)

Figure 2. (**a**) Grading curve; (**b**) Triaxial apparatus. Grain size distribution and triaxial apparatus for tested granular materials.

Table 1. The basic characteristics of grading curves.

	Gc1	**Gc2**	**Gc3**	**Gc4**	**Gc5**
Coefficient of uniformity	2	5	10	20	40
Curvature coefficient	1.17	1.44	1.68	1.97	2.30
Maximum dry density (g/cm^3)	1.71	1.78	1.94	2.12	2.23
Minimum dry density (g/cm^3)	1.47	1.57	1.68	1.78	1.79

The experimental program comprised a consolidated drained triaxial shear test with an initial sample size of a 100 mm diameter and a 200 mm height. The specimen preparation and loading process were carried out step by step with reference to the specification of soil test (SL237-1999) [26]. Aggregates were weighed separately and mixed together before being split into five equal portions. Each portion was then compacted inside a split cylindrical mould. The monotonic shearing rate of displacement was determined

to be 0.6 mm/min. Before shearing, the sample was saturated by allowing water to pass through the base of the triaxial cell under a back pressure of 50 kPa until Skempton's B-value exceeded 0.95. In order to analyse the particle breakage, four different relative densities (i.e., Rd = 0.6, 0.7, 0.8 and 0.9 of grading curve Gc3) and five kinds of grading curves (i.e., Gc1, Gc2, Gc3, Gc4 and Gc5 in Rd = 0.9) were selected under four values of confining pressures (i.e., σ3 = 0.2, 0.4, 0.6 and 0.8 MPa). A load cell and pore-pressure sensor were used to measure the deviator load and drainage volume, respectively, through the electronic display system. All the tests were conducted up to a maximum axial strain of 25%.

3. Analysis of Test Results

3.1. Particle Breakage under Different Relative Density

The particle size distribution of natural granular materials in this study can be described by using the Talbot grading curve [27]. Blasting granular materials can meet the Talbot grading curve by adjusting the blasting parameters, and subsequently it will represent fractal characteristics and be easier to achieve the maximum dry density. The proportion of particle mass can be calculated by using the following formula:

$$\frac{W(\delta > d)}{W_0} = 1 - F(d) \tag{1}$$

$$F(d) = \left(\frac{d}{d_M}\right)^{3-D} \tag{2}$$

where d is the diameter of the particle, $W(\delta > d)$ is the mass of particle with diameter larger than d, W_0 is the total mass of granular materials, d_M is the particle maximum diameter, $F(d)$ is the mass ratio of granular materials with diameter less than d and D is the fractal dimension.

The stress–strain behaviour of granular materials tested at different Rd of 0.6, 0.7, 0.8 and 0.9 is shown in Figure 3, respectively. The peak shear stress increases (such as 2.42, 2.43, 2.53 and 2.78 MPa) with the increase in Rd, for a given effective confining pressure (σ_3 = 0.6 MPa). However, the residual shear stresses remain approximately the same for the different Rd for a given confining pressure. The stress–strain behaviour of granular materials transforms from a strain hardening type to a strain softening type for all the tested specimens. As the shear strain further increases, the residual shear stresses corresponding to the rockfill with different Rd become stable. All the granular materials tested in this study exhibit characteristics similar to those observed by Lade [28] for sands. This can be attributed to the observation that the greater the relative density, the greater the interlocking between the particles; and the greater the loading, the greater was the peak strength of the specimen under the same confining pressure. As the load increased, particle breakage occurred, the interlocking force between particles would decrease and the shear strength would decrease.

Furthermore, a general compression followed by the dilatancy can be observed in all granular materials tested at low confining pressures. Granular materials gradually became more compressive with the increasing confining pressure. The larger the relative density was, the dilatancy became much more pronounced. The volumetric strain became stable as the strain increased, whereas it decreased as the relative density increased. This can be attributed to the enhanced sliding rather than rotation between aggregates when the compressive pressure increases.

At the monotonic loading test, the grading curve of granular materials changed due to the occurrence of particle breakage. Thus, the fractal dimensions of each grading curve changed after each test. Figure 4 shows the fractal dimension obtained under different confining pressures after monotonic loading. There is a good linear relationship between $\ln F(d)$ and $\ln(d/d_M)$ after loading under different confining pressures. The values of R^2 are larger than 0.97, and the Root mean squared Error (Re) is smaller than 0.23. The fractal

dimension increases with confining pressure during of particle breakage. For example, the fractal dimension increases from 2.33 (σ_3 = 0.2 MPa) to 2.37 (σ_3 = 0.8 MPa) when relative density Rd = 0.6. However, relative density has little influences on the fractal dimension, especially under higher relative density. For example, the fractal dimensions are almost the same for Rd = 0.8 and 0.9.
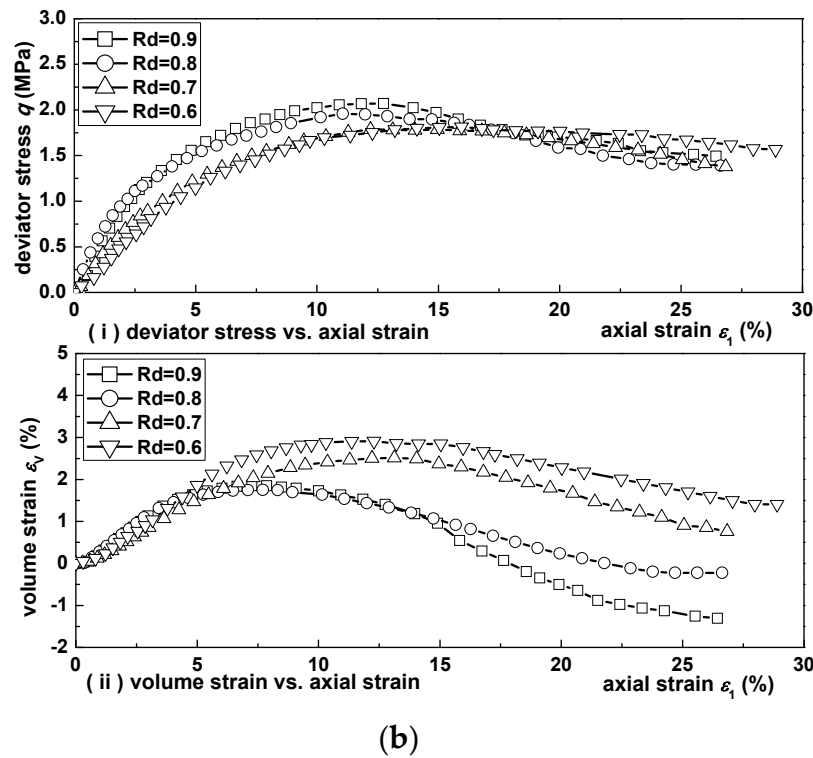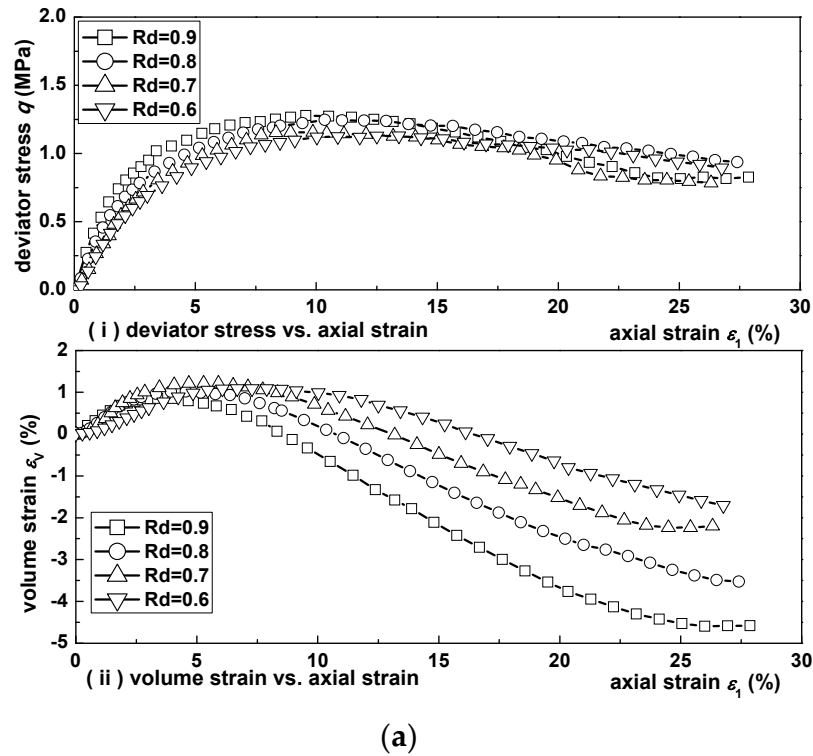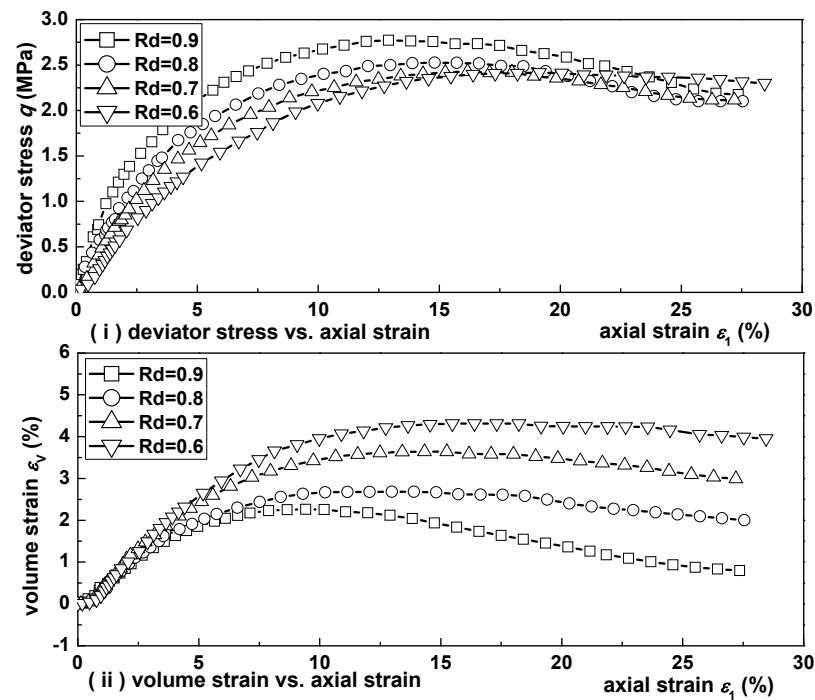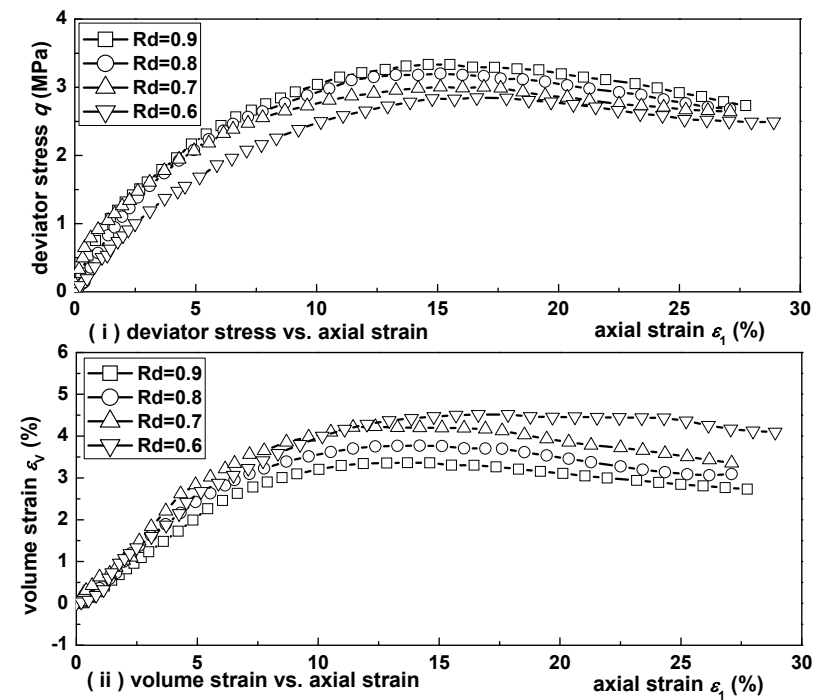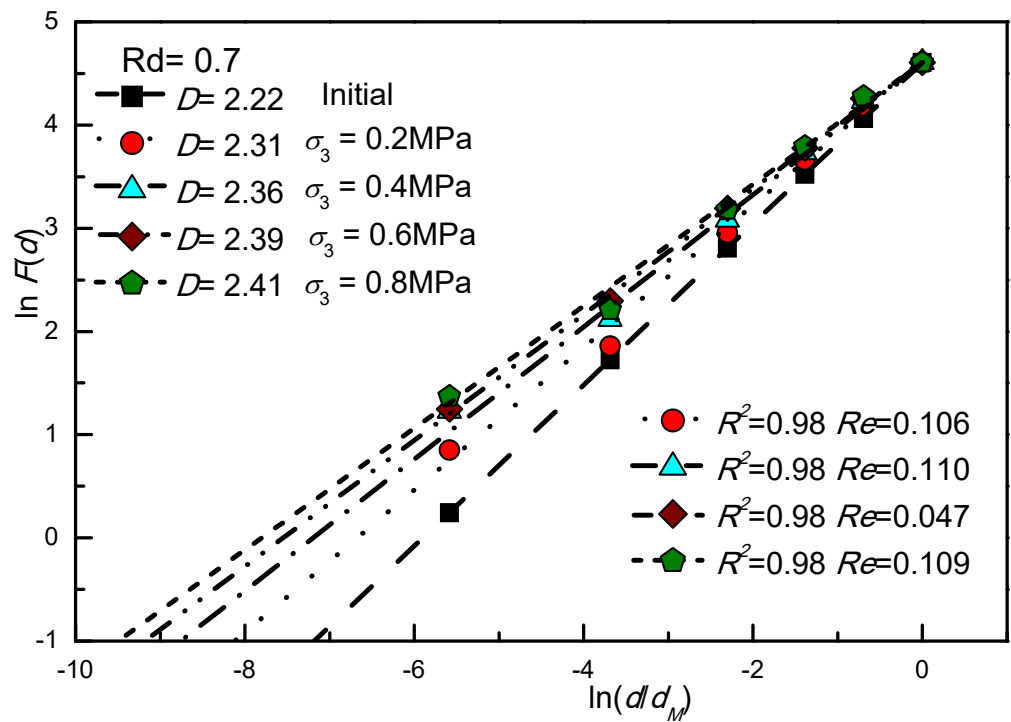

Figure 3. *Cont.*

Figure 3. (**a**) confining pressure of 0.2 MPa; (**b**) confining pressure of 0.4 MPa; (**c**) confining pressure of 0.6 MPa; (**d**) confining pressure of 0.8 MPa. Stress–strain behaviour of granular materials under different confining pressures.
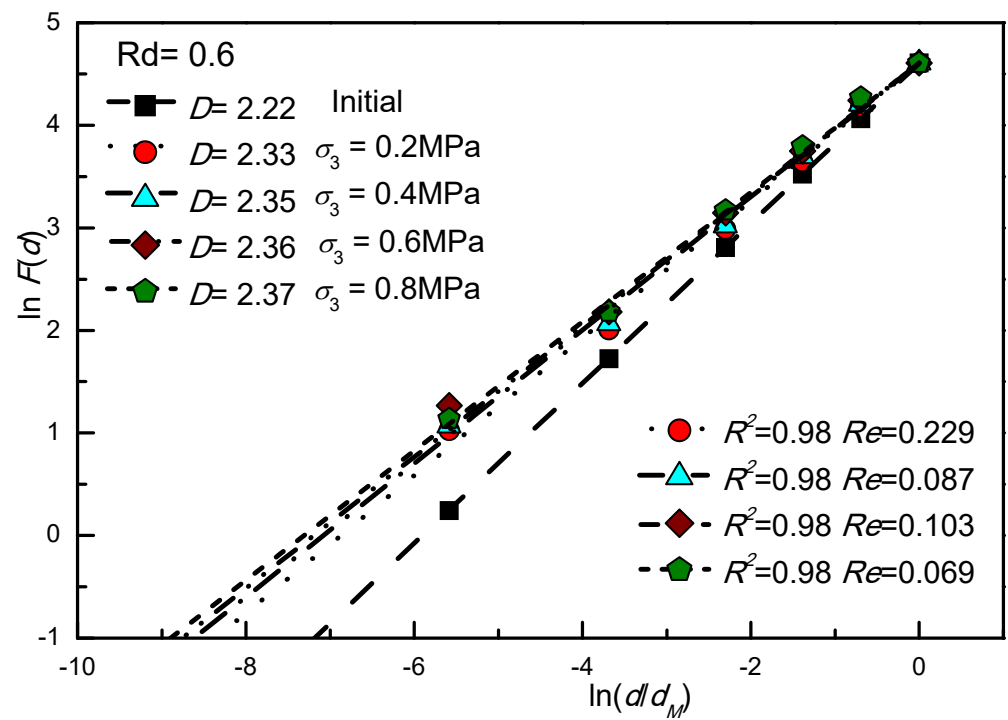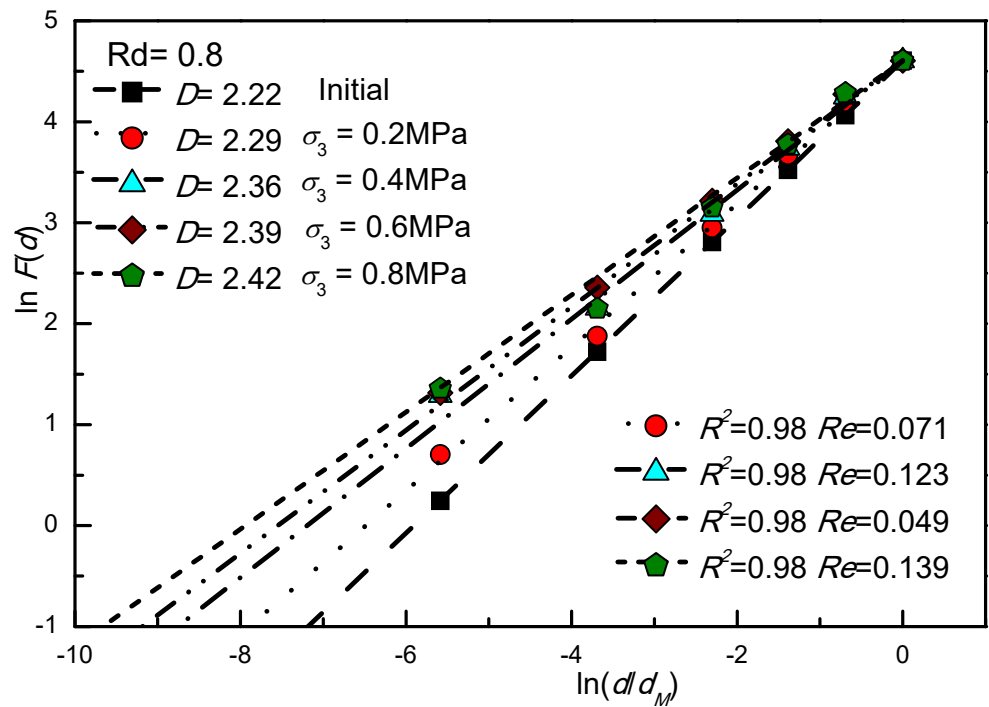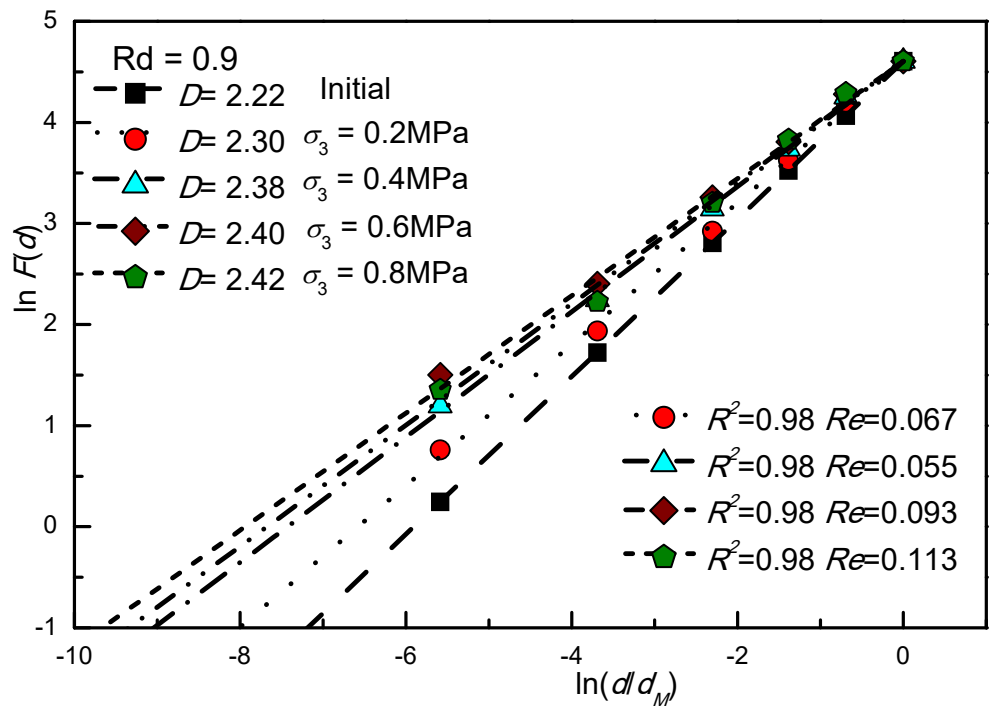
(**a**)

(**b**)

Figure 4. *Cont.*

(**c**)

(**d**)

Figure 4. (**a**) Rd = 0.6; (**b**) Rd = 0.7; (**c**) Rd = 0.8; (**d**) Rd = 0.9. Grading curves of different relative densities.

The extent of particle breakage during monotonic drained shearing is further assessed. In this study, the breakage ratio Bg presented by Marsal [29] is used for analysis, which can be expressed as the following:

$$B_g = \sum |P_{test} - P_{ini}| \tag{3}$$

where P_{test} is percentage by mass of particles after the test, and P_{ini} is percentage by mass of particles before the test.

The evolution of breakage ratio at different confining pressures is shown in Figure 5. According to the results, breakage ratio increases with an increase in confining pressure. The relationship between breakage ratio and confining pressure can be simulated by using a power function. The larger the relative density is, the greater the interlocking force between the particles is. Moreover, at the same axial strain level, the larger the shear stress is, the larger the particle breakage ratio is. With the increase of the relative density, breakage ratio increases. A power function is found to be able to fit well the relationship between breakage ratio, relative density and confining pressure, such that:

$$B_g = k_1 \left(\frac{\sigma_3}{p_a} Rd \right)^n \tag{4}$$

where k_1 and n are model parameters, determined to be 6.36 and 0.46, respectively; p_a (= 101 kPa) is the atmospheric pressure.
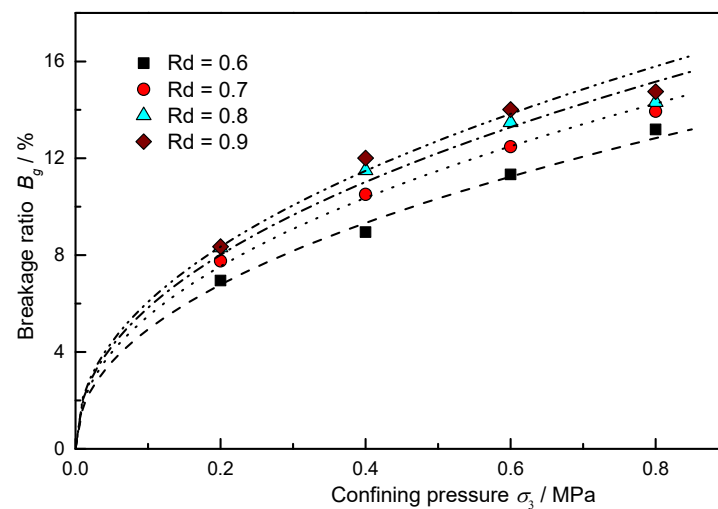
(**a**)
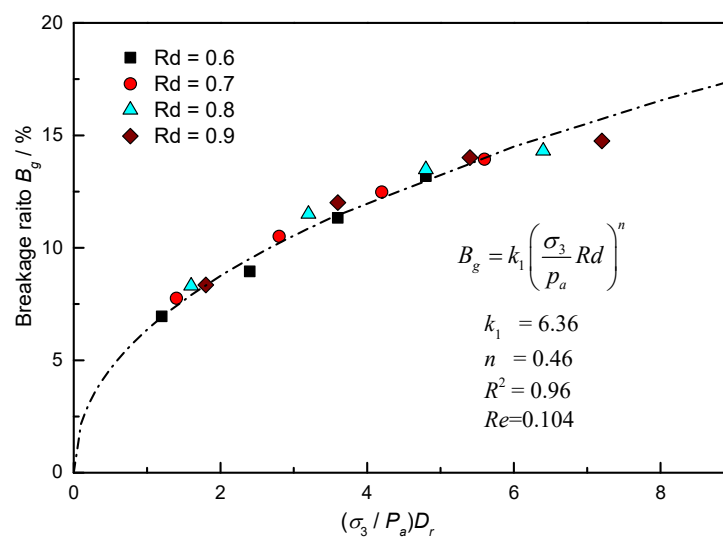
(**b**)

Figure 5. (**a**) Breakage ratio vs. confining pressure; (**b**) Breakage ratio vs. normalized confining pressure. Particle breakage of different relative densities.

3.2. Particle Breakage under Different Grading Curve

Figure 6 shows the fractal dimension under different confining pressures after monotonic loading. There is also a good linear relationship between $\ln F(d)$ and $\ln(d/d_M)$ after loading at different confining pressures. Compared with those under different relative densities, the initial fractal dimension has great influences on the final fractal dimensions obtained under different confining pressures, as shown in Figure 7. It can also be observed that under low confining pressures, granular materials can undergo significant particle breakage. The smaller the fractal dimension is, the more significant the particle breakage extent will be. The larger the fractal dimension is, the greater the content of fine particles, the smaller the particle crushing rate during shearing and the smaller the effect of confining pressure on particle crushing. As the confining pressure increases, it tends to the final limit fractal dimension 2.6 [30].

The evolution of the breakage ratio at different confining pressures is shown in Figure 8. Unlike the relationship between the relative density and particle breakage ratio in direct proportion, the coefficient of uniformity is inversely proportional to the particle breakage ratio. The greater the coefficient of uniformity, the smaller is the particle breakage ratio. A normalized power function is also found to fit well the relationship between breakage ratio, relative density, uniform coefficient and confining pressure. The expression is shown as follows:

$$B_g = k_2 \left(\frac{\sigma_3}{p_a C_u} Rd \right)^n \tag{5}$$

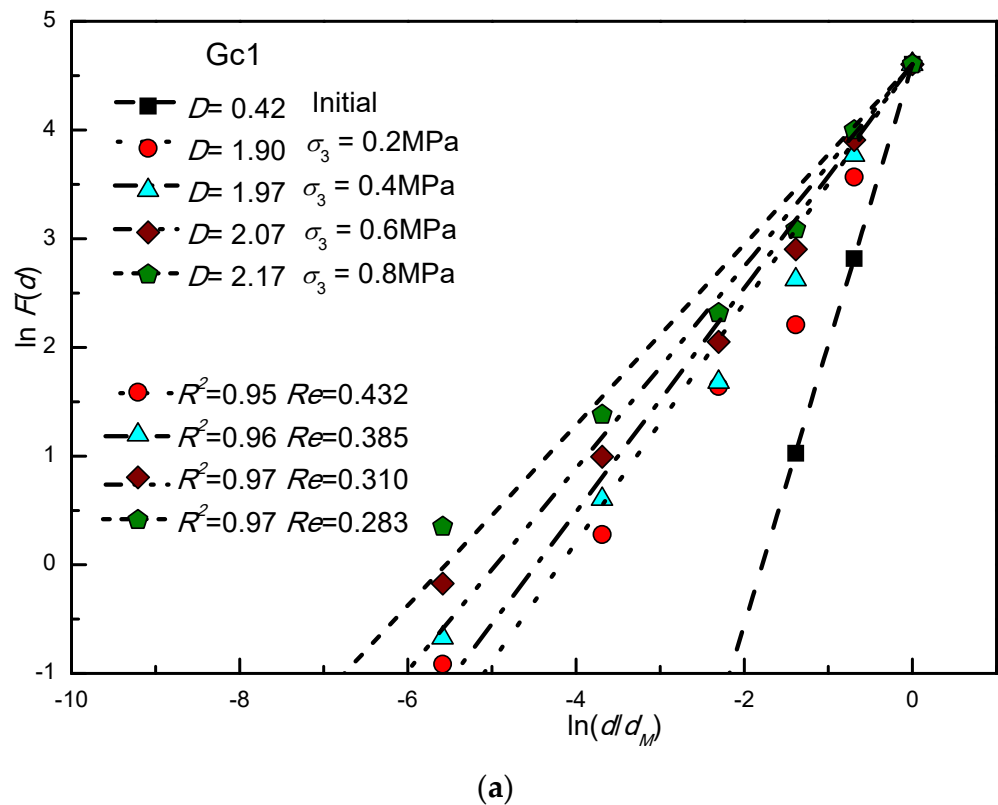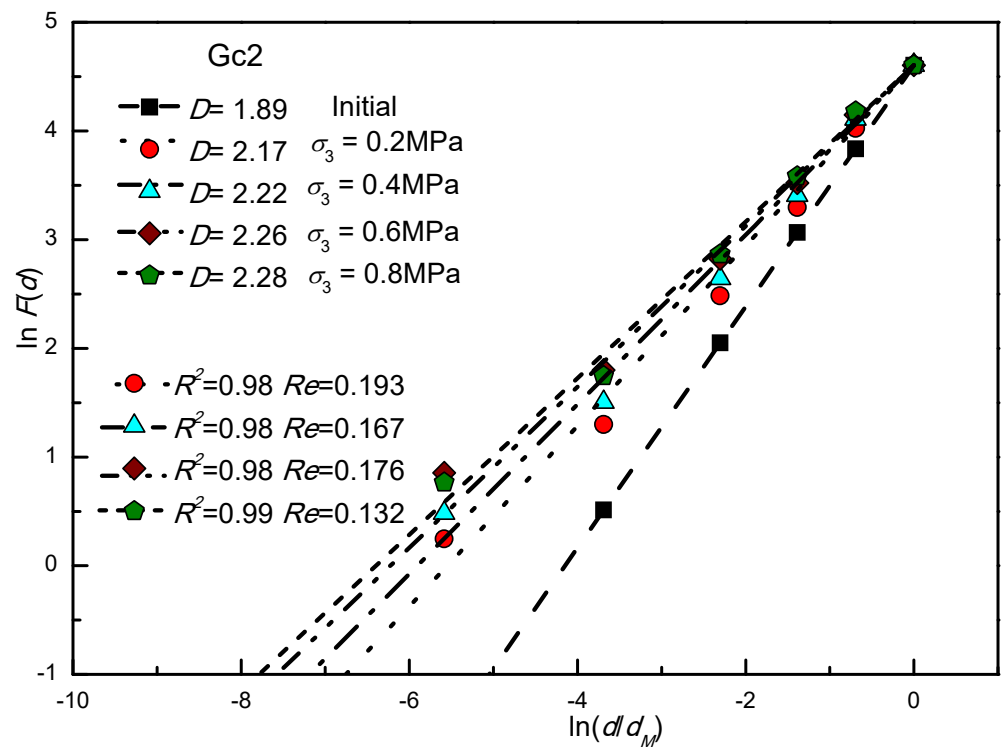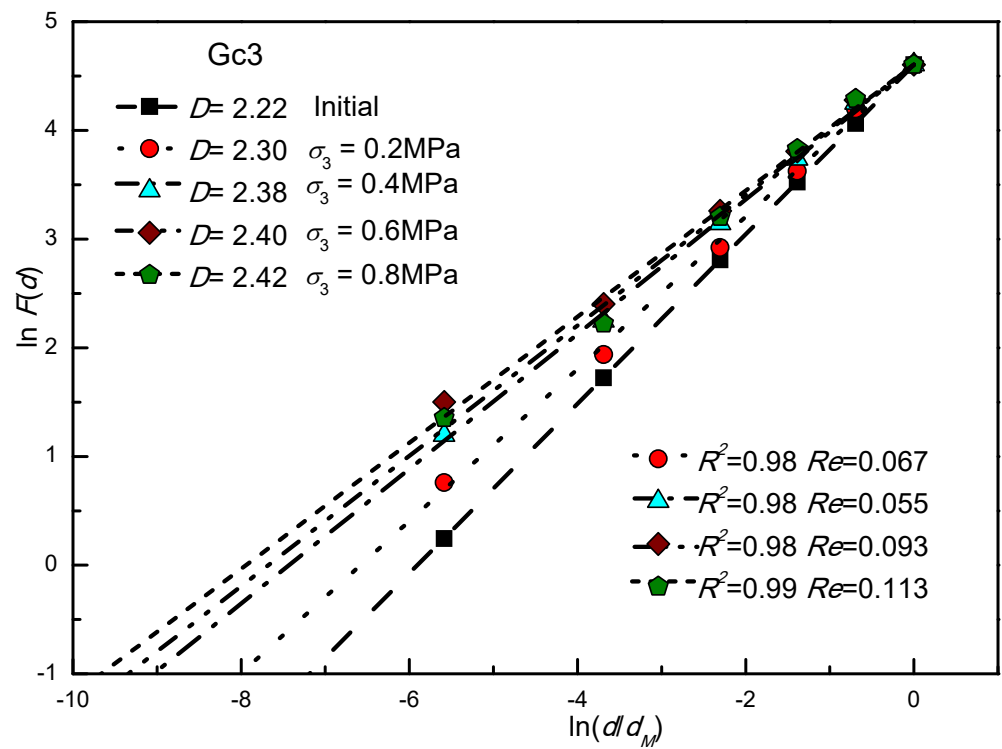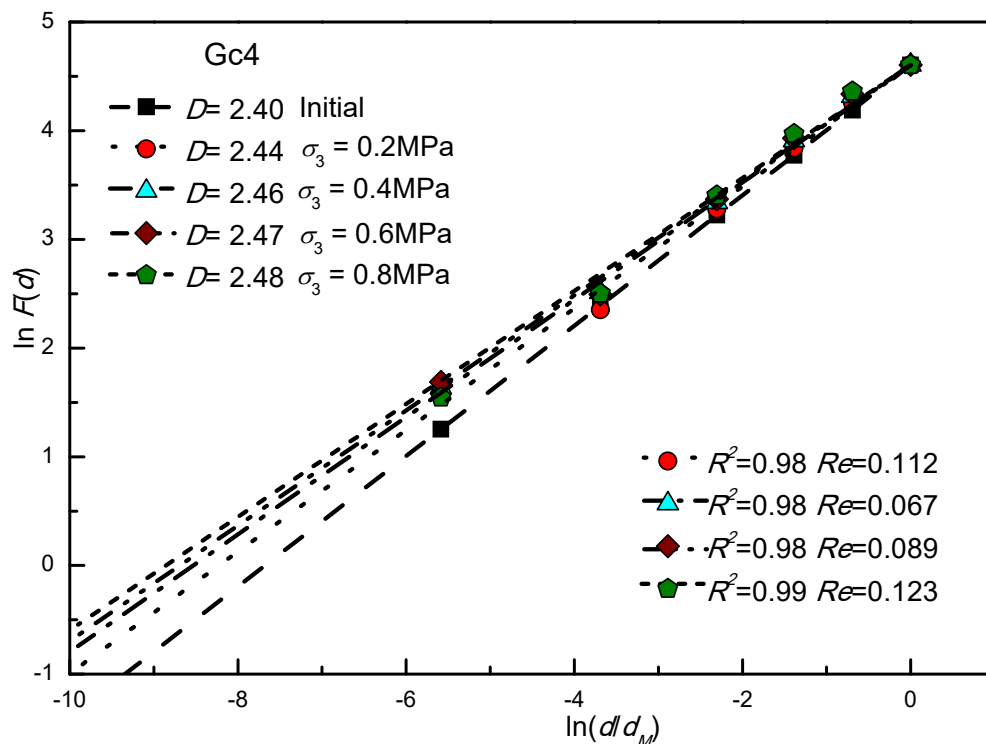where k_2 and n are model parameters, determined to be 19.1 and 0.46, respectively.

(a)

Figure 6. *Cont.*

(**b**)

(**c**)

Figure 6. *Cont.*

(**d**)
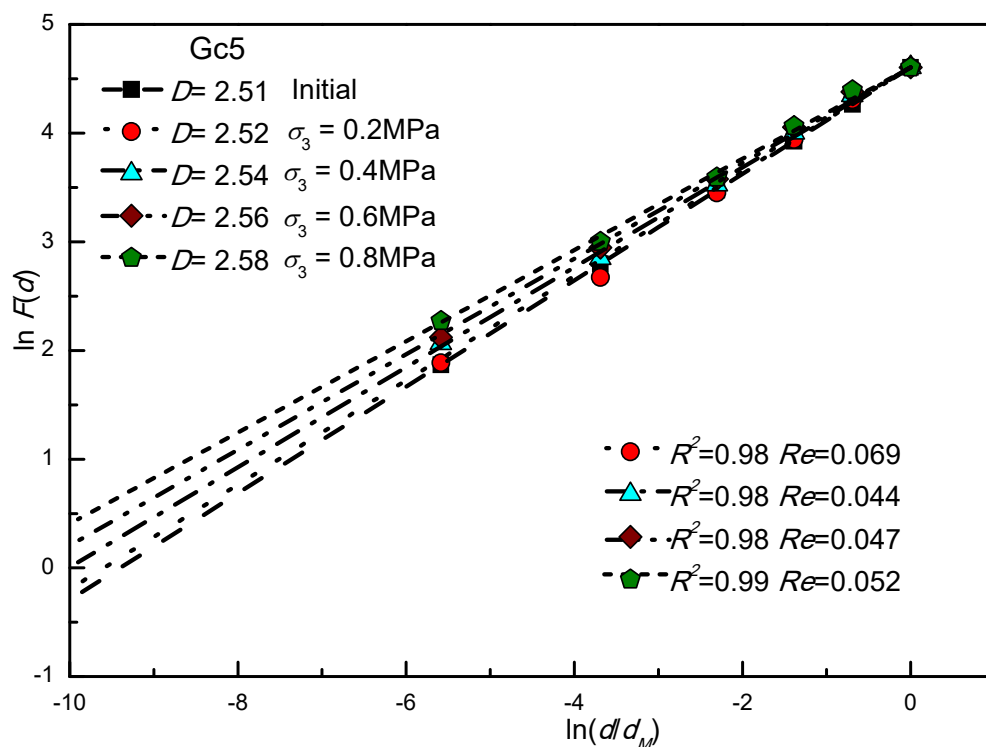
(**e**)

Figure 6. (**a**) Grading curves of Gc1; (**b**) Grading curves of Gc2; (**c**) Grading curves of Gc3; (**d**) Grading curves of Gc4; (**e**) Grading curves of Gc5. Grading curves of different grading curves.

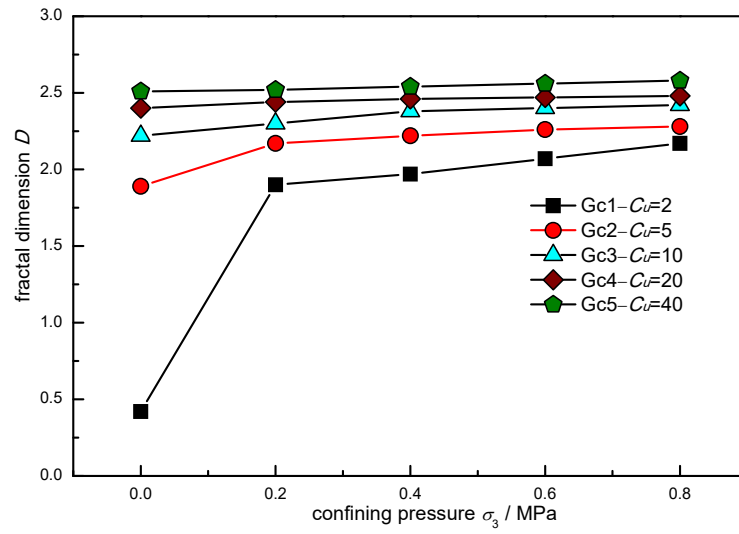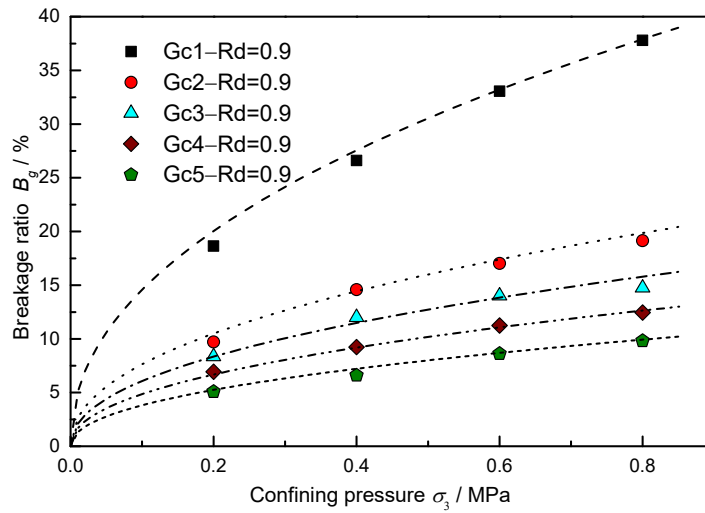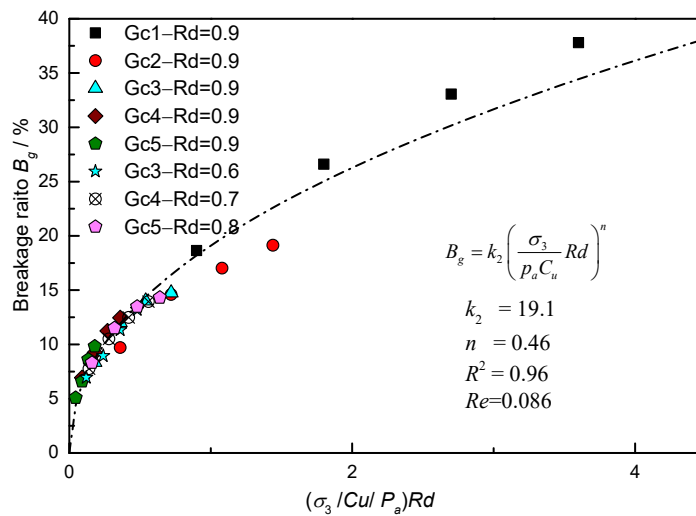**Figure 7.** Fractal dimension of different grading curves.

(**a**)

(**b**)

Figure 8. (**a**) Breakage ratio vs. confining pressure; (**b**) Breakage ratio vs. normalized confining pressure. Particle breakage of different grading curves.

Median diameter d_{50} is an important soil grading curve index. The larger the median diameter, the higher the shear strength and the more obvious is the shear expansion effect [31]. Figure 9 shows the relationship between the particle breakage ratio with d_{50} under different confining pressures after monotonic loading. The greater d_{50}, the greater is the particle breakage ratio. According to previous research, the confining pressure effect can be expressed by a power function. A normalized power function is also found to fit well the relationship between breakage ratio, d_5 and confining pressure. The expression is shown as follows:

$$B_g = k_3 \frac{d_{50}}{d_M} \left(\frac{\sigma_3}{p_a} \right)^{n_3} \tag{6}$$

where k_2 and n_3 are model parameters, determined to be 16.5 and 0.46 (which is the same as the previous value of the coefficient of uniformity).
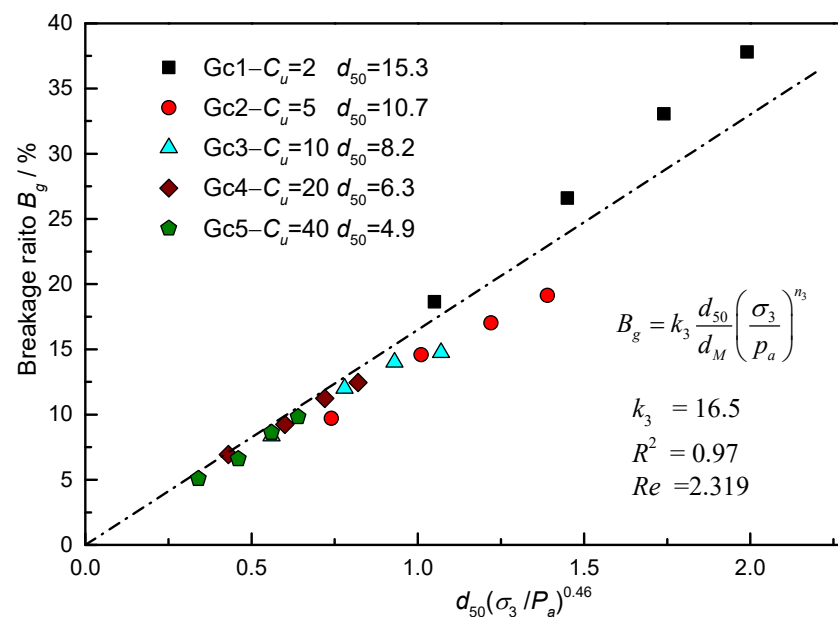
Figure 9. Breakage ratio vs. median diameter under different confining pressures.

The particle breakage is related to the relative density, uniform coefficient and stress level of the granular materials. Figure 10 shows the percentage increment of particle weight, ΔF, under different confining pressures.

$$\Delta F = P_{test} - P_{ini} \tag{7}$$

During the shear process, the percentage increment in the range of 5–10 mm is found to be almost the same under different confining pressures except the grading curve Gc1. However, the percentage increment in the range of 10–20 mm shows considerable increase with an increase in the confining pressure, relative density and decrease in coefficient of uniformity. Compared with particle percentage increment, particle breakage mainly occurs in large particles during shear tests, indicating that the particles in the range of 5–10 mm exhibit limited breakage, because the large particles can break into middle and small particles. However, further mechanisms should be analysed, combined with discrete element model (DEM) simulations.
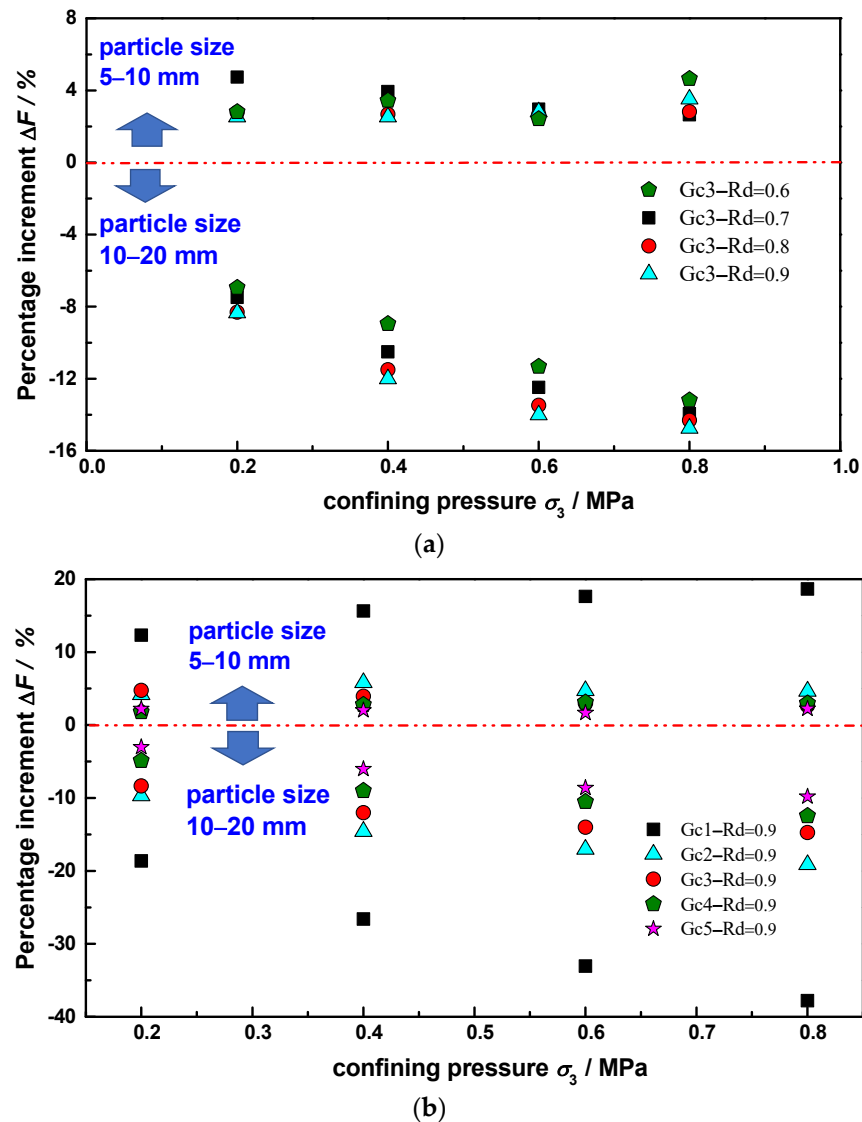
Figure 10. (**a**) Different relative density; (**b**) different grading curves. Particle percentage increment ($\Delta F > 0$, particle percentage increasing).

4. Conclusions

In this study, the influence of relative density and grading curve on the particle breakage of granular material was investigated. A series of consolidated drained triaxial tests were performed on granular materials subjected to monotonic loading. The major findings of this study are summarized below:

(1) The particle size distribution exhibited good fractal characteristics after monotonic loading of rockfill at different confining pressures. The fractal dimension increased with the increase in confining pressure. The coefficient of uniformity exhibited a greater effect on the fractal dimension than relative density.

(2) During the shearing process, the main occurrence of breakage was found to be in large particles. The extent of particle breakage increased with the increase of confining pressure and relative density, whereas it decreased with an increase in the coefficient of uniformity, which can be well described by a normalized power function. The relationship between the breakage ratio and the median diameter can be described by a linear function.

(3) The conclusions are mainly based on the results after the test. In fact, fractal dimension and particle breakage change with axial loading. Future research should focus on the

results during the shear test. The relationship between fractal dimension and particle breakage with shear modulus and volume strain should be investigated.

Informed Consent Statement: Informed consent was obtained from all subjects involved in the study. Written informed consent has been obtained from the patient(s) to publish this paper.

Data Availability Statement: All data, models, and code generated or used during the study appear in the submitted article.

Conflicts of Interest: The authors declare no conflict of interest.

References

1. Liu, J.; Liu, F.; Kong, X.; Yu, L. Large-scale shaking table model tests on seismically induced failure of Concrete-Faced Rockfill Dams. *Soil Dyn. Earthq. Eng.* **2016**, *82*, 11–23. [CrossRef]
2. Yang, G.; Yu, T.; Yang, X.; Han, B. Seismic Resistant Effects of Composite Reinforcement on Rockfill Dams Based on Shaking Table Tests. *J. Earthq. Eng.* **2017**, *21*, 1010–1022. [CrossRef]
3. Wei, K.M.; Zhu, S.; Yu, X.H. Influence of the scale effect on the mechanical parameters of coarse-grained soils. *Iran. J. Sci. Technol.—Trans. Civ. Eng.* **2014**, *38*, 75–84.
4. Huang, J.Y.; Hu, S.S.; Xu, S.L.; Luo, S.N. Fractal crushing of granular materials under confined compression at different strain rates. *Int. J. Impact Eng.* **2017**, *106*, 259–265. [CrossRef]
5. Xu, M.; Song, E.; Chen, J. A large triaxial investigation of the stress-path-dependent behavior of compacted rockfill. *Acta Geotech.* **2012**, *7*, 167–175. [CrossRef]
6. Jia, Y.; Xu, B.; Chi, S.; Xiang, B.; Xiao, D.; Zhou, Y. Particle Breakage of Rockfill Material during Triaxial Tests under Complex Stress Paths. *Int. J. Geomech.* **2019**, *19*, 04019124. [CrossRef]
7. Yan, W.; Dong, J. Effect of particle grading on the response of an idealized granular assemblage. *Int. J. Geomech. ASCE.* **2011**, *11*, 276–285. [CrossRef]
8. Yang, J.; Luo, X.D. Exploring the relationship between critical state and particle shape for granular materials. *J. Mech. Phys. Solids.* **2015**, *84*, 196–213. [CrossRef]
9. Ovalle, C.; Frossard, E.; Dano, C.; Hu, W.; Maiolino, S.; Hicher, P.Y. The effect of size on the strength of coarse rock aggregates and large rockfill samples through experimental data. *Acta Mech.* **2014**, *225*, 2199–2216. [CrossRef]
10. Varadarajan, A.; Sharma, K.G.; Venkatachalam, K.; Gupta, A.K. Testing and Modeling Two Rockfill Materials. *J. Geotech. Geoenviron. Eng.* **2003**, *129*, 206–218. [CrossRef]
11. Yang, G.; Yan, X.; Nimbalkar, S.; Xu, J. Effect of Particle Shape and Confining Pressure on Breakage and Deformation of Ar-tificial Rockfill. *Int. J. Geosynth. Gr. Eng.* **2019**, *5*, 15. [CrossRef]
12. Li, X.; Liu, J.; Li, J. Fractal dimension, particle shape, and particle breakage analysis for calcareous sand. *Bull. Eng. Geol. Environ.* **2022**, *81*, 106. [CrossRef]
13. Xiao, Y.; Liu, H.; Chen, Y.; Jiang, J.; Zhang, W. Testing and modeling of the state-dependent behaviors of rockfill material. *Comput. Geotech.* **2014**, *61*, 153–165. [CrossRef]
14. Wang, C.; Ding, X.; Xiao, Y.; Peng, Y.; Liu, H. Effects of relative densities on particle breaking behaviour of non-uniform grading coral sand. *Powder Technol.* **2021**, *382*, 524–531. [CrossRef]
15. USACE. *General Design and Construction Considerations for Earth and Rock-Fill Dams*; USACE: Washington, DC, USA, 2004; 130 p.
16. Honkanadavar, N.P.; Sharma, K.G. Testing and Modeling the Behavior of Riverbed and Blasted Quarried Rockfill Materials. *Int. J. Geomech.* **2014**, *14*, 04014028. [CrossRef]
17. Ueng, T.; Chen, T. Energy aspects of particle breakage in drained shear of sands. *GeoTechnology* **2000**, *50*, 65–72. [CrossRef]
18. Nakata, Y.; Kato, Y.; Hyodo, M.; Hyde, A.F.L.; Murata, H. one-dimensional compression behaviour of uniformly graded sand related to single particle crushing strength. *Soils Found.* **2001**, *41*, 39–51. [CrossRef]
19. Shi, D.; Zheng, L.; Xue, J.; Sun, J. DEM Modeling of Particle Breakage in Silica Sands under One-Dimensional Compression. *Acta Mech. Solida Sin.* **2016**, *29*, 78–94. [CrossRef]
20. Lade, P.V.; Bopp, P.A. Relative density effects on drained sand behavior at high pressures. *Soils Found.* **2005**, *45*, 1–13.

21. Miura, N.; Yamanouchi, T. Effect of water on the behavior of quartz-rich sand under high stresses. *Soils Found.* **1975**, *15*, 23–34. [CrossRef]
22. Kikumoto, M.; Wood, D.M.; Russell, A. Particle Crushing and Deformation Behaviour. *Soils Found.* **2010**, *50*, 547–563. [CrossRef]
23. Indraratna, B.; Sun, Y.; Nimbalkar, S. Laboratory Assessment of the Role of Particle Size Distribution on the Deformation and Degradation of Ballast under Cyclic Loading. *J. Geotechnol. Geoenviron. Eng.* **2016**, *142*, 04016016. [CrossRef]
24. Soroush, A.; Jannatiaghdam, R. Behavior of rockfill materials in triaxial compression testing. *Int. J. Civ. Eng.* **2012**, *10*, 153–161.
25. Yang, G.; Jiang, Y.; Nimbalkar, S.; Sun, Y.; Li, N. Influence of Particle Size Distribution on the Critical State of Rockfill. *Adv. Civ. Eng.* **2019**, *2019*, 8963971. [CrossRef]
26. Ministry of Water Resources of the PRC. *Specification of Soil Test*; China Water Conservancy Hydropower Publishing House: Beijing, China, 1999.
27. Ochiai, M.; Ozao, R.; Yamazaki, Y.; Holz, A. Self-similarity law of particle size distribution and energy law in size reduction of solids. *Phys. A Stat. Mech. Its Appl.* **1992**, *191*, 295–300. [CrossRef]
28. Lade, P.V.; Yamamuro, J.A.; Bopp, P.A. Relative density effects on drained and undrained strengths of sand at high pressures. In Proceedings of the 16th International Conference on Soil Mechanics and Geotechnical Engineering, Osaka, Japan, 12–16 September 2005; pp. 537–541.
29. Marsal, R.J. Large scale testing of rockfill materials. *Soil Mech Found Div.* **1967**, *93*, 27–43. [CrossRef]
30. Einav, I. Breakage mechanics—Part I: Theory. *J. Mech. Phys. Solids.* **2007**, *55*, 1274–1297. [CrossRef]
31. Zhu, Z.; Zhang, F.; Dupla, J.; Canou, J.; Foerster, E. Investigation on the undrained shear strength of loose sand with added materials at various mean diameter ratios. *Soil Dyn. Earthq. Eng.* **2020**, *137*, 106276. [CrossRef]